
Article:
Donovan, K., Harrison, P. and Kelsall, R.W. (1998) Stark ladders as tunable far-infrared emitters. Journal of Applied Physics, 84 (9). pp. 5175-5179. ISSN: 1089-7550

https://doi.org/10.1063/1.368810

Stark ladders as tunable far-infrared emitters

K. Donovan,[a] P. Harrison, and R. W. Kelsall
Institute of Microwaves and Photonics, School of Electronic and Electrical Engineering, University of Leeds, Leeds LS2 9JT, United Kingdom

(Received 31 March 1998; accepted for publication 15 July 1998)

A superlattice of GaAs/$Ga_{1-x}Al_xAs$ quantum wells forms a Stark ladder under the influence of a perpendicular electric field. A two level incoherent emitter system, formed by radiative intersubband transitions between adjacent wells, is investigated as a tunable far-infrared radiation source. Intersubband transition rates are calculated at 4, 77, and 300 K for applied fields from 0 to 40 kV cm^{-1}. It is shown that the quantum efficiency of the radiative emission reaches a maximum at low temperatures for a field of 32 kV cm^{-1}. Under these conditions the emission wavelength is 38 μm with an estimated power output of 1.1 mW. © *1998 American Institute of Physics.* [S0021-8979(98)04620-9]

I. INTRODUCTION

Recently there have been developments of semiconductor emitters based on intersubband transitions between conduction band states, in particular quantum cascade lasers operating in the mid-infrared.[1] Additionally, the use of an electric field to tune the output wavelength has been investigated[2] and there have been reports of tunable emission in the far-infrared region (1–10 THz or 30–300 μm).[3] In this article a theoretical study is made of a two level emitter based on intersubband transitions between the conduction band states of adjacent wells in a Stark ladder. The main advantage of this two level system is the range of tunable output.

Intersubband transitions can take place via several mechanisms in semiconductor systems.[4] Obviously the most important electron transitions in a system to be used as a terahertz emitter are those which result in the emission of photons—the radiative transitions. However, nonradiative transitions may also take place via electron–phonon scattering and electron–electron scattering.[5,6] These nonradiative transitions are undesirable because they compete with radiative emission and hence reduce the efficiency, even though in the design of lasers they can be used to good effect in creating population inversion.[7]

A possible system that would fulfil the criteria for a tunable far-infrared emitter based on intersubband transitions is a Stark ladder structure. A Stark ladder is formed when an electric field is applied to a superlattice. The field changes the potential of adjacent wells, resulting in the formation of localized energy states, or subbands.[8] Electron transitions between subbands can result in the emission of photons. One important feature of the Stark ladder is that the subband separation is proportional to the applied electric field, which means that the intersubband separation, and therefore the photon energy, can be tuned.

To obtain coherent emission, a population inversion must be achieved between two subbands, and this is only possible in a system with three or more levels. The Stark ladder structure is a two level system so all emission would be incoherent. However, an advantage of the system suggested here is that the subband separation can be tuned from 5 to 37 meV, resulting in a range of emission wavelengths tunable from 33 to 248 μm.

II. THEORY

When an electric field F is applied to a superlattice, it introduces an extra term to the potential, $-eFz$.[9] Using the envelope function and effective mass approximations the Schrödinger equation would be written as

$$\left(\frac{-\hbar^2}{2}\frac{\partial}{\partial z}\frac{1}{m^*}\frac{\partial}{\partial z}+V(z)-eF(z-z_o)\right)\psi=E\psi, \qquad (1)$$

where z_o is the origin of the field at the center of the quantum well defined by the one-dimensional potential $V(z)$. This equation was solved using a numerical shooting technique.[10] The material parameters of effective mass and band discontinuity were assumed to be independent of temperature, with the values taken from Adachi.[11] In particular, $m^*(\mathrm{GaAs})=0.067m_0$, $m^*(Ga_{0.8}Al_{0.2}As)=0.836m_0$, $V(\mathrm{GaAs})=0$, and $V(Ga_{0.8}Al_{0.2}As)=167$ meV.

This article presents a study of a five well structure of 50 Å $Ga_{0.8}Al_{0.2}As$ barriers and 50 Å GaAs wells in which the intersubband separation in the Stark ladder regime lies in the far-infrared region. This is demonstrated by the graph of subband minima versus field shown in Fig. 1. It can be seen that the intersubband separation is proportional to the field for fields $\geqslant 7$ kV cm^{-1}, enabling the output wavelength to be easily tuned. At smaller fields the wave functions are not very well localized and the system does not exhibit Stark ladder behavior.

Figure 2 displays the Stark ladder effect when an electric field is applied to a multiple quantum well. It can be seen that the wave functions are localized in each well and the energy separations between them form an equally spaced ''ladder.''

[a]Electronic mail: phykd@sun.leeds.ac.uk

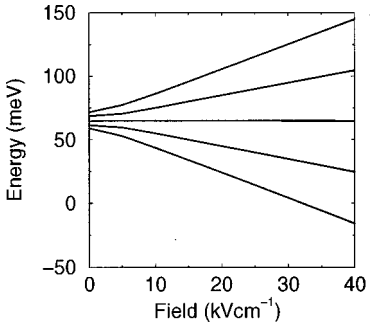

FIG. 1. The effect of electric field on the intersubband separation of a five well system.

The numerical wave functions were used to calculate the radiative and nonradiative transition rates between the Stark ladder states; the aim is to determine the quantum efficiency of the system. This will determine its feasibility as a device. Bulk phonon modes were assumed for the calculation of the electron–phonon transition rates. The electron–electron scattering and radiative rates were calculated using the approach of Smet *et al.*[12] The longitudinal optical (LO) phonon energy is 36 meV in GaAs (corresponding to a wavelength of 34 μm) thus implying that LO phonon emission (which represents a loss process) will be suppressed for subband separations less than 36 meV.[4]

Scattering rates were calculated for all intersubband transitions in the five well Stark ladder from level $|n+1\rangle \rightarrow |n\rangle$, i.e., $5\rightarrow4$, $4\rightarrow3$, $3\rightarrow2$, and $2\rightarrow1$ at 4, 77, and 300 K for an applied field of 40 kV cm^{-1}. These are displayed for 4 and 300 K in Tables I and II, respectively. To decrease computational time, future calculations were performed only for the transitions between levels 4 and 3 (later labeled levels 2 and 1). This is justified because it can be seen from Tables I and II that the scattering rates for each of the four transitions between initial and final states are almost identical, thus showing that this system can be used—to a very good approximation—as a model of an infinite superlattice. The only exceptions are the transition rates from level 2 to level 1. These are slightly different from the other rates because of end effects (the wave function from the lowest level in the Stark ladder is modified by the adjacent barrier potential, as shown in Fig. 2).[13] All transition rate calculations, radiative and nonradiative, were repeated at intervals of 5 kV cm^{-1} from 0 to 40 kV cm^{-1} at temperatures of 4, 77, and 300 K.

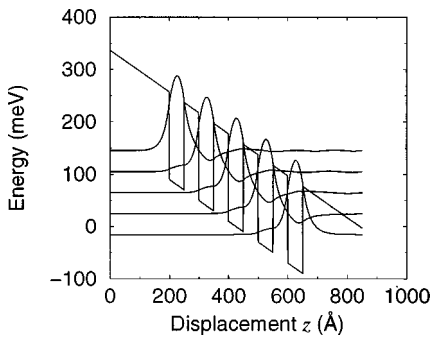

FIG. 2. A schematic representation of the energy levels and wave functions in the Stark ladder regime.

TABLE I. Scattering rates at 4 K with an applied field of 40 kV cm^{-1}.

Transition	$1/\tau_{LO}$	$1/\tau_{AC}$	$1/\tau_{ee}$
$5\rightarrow4$	3.642×10^{11}	2.081×10^{8}	8.990×10^{7}
$4\rightarrow3$	3.660×10^{11}	2.064×10^{8}	8.899×10^{7}
$3\rightarrow2$	3.652×10^{11}	2.057×10^{8}	8.834×10^{7}
$2\rightarrow1$	3.485×10^{11}	1.990×10^{8}	8.342×10^{7}

There are three possible mechanisms for electron–electron scattering from the initial to the final energy state: $22\rightarrow11$, $22\rightarrow21$, and $21\rightarrow11$, where 2 and 1 are the initial and final subbands, respectively. The last two processes are Auger type transitions which only occur when an electric field is applied to the superlattice. This is because there is an asymmetry introduced to the superlattice potential on application of a field; a condition necessary for Auger transitions to take place.[14]

The total electron–electron scattering rate ($1/\tau_{ee}$) for a two level system is the sum of all three mechanisms:

$$\frac{1}{\tau_{ee}}=\frac{1}{\tau_{2221}}+\frac{1}{\tau_{2211}}+\frac{1}{\tau_{2111}}, \tag{2}$$

where $1/\tau_{2221}$, $1/\tau_{2211}$, and $1/\tau_{2111}$ are the transition rates for the electron–electron scattering mechanisms $22\rightarrow21$, $22\rightarrow11$, and $21\rightarrow11$, respectively. The internal quantum efficiency of the Stark ladder system is given by

$$\eta=\frac{1}{\tau_r}\left(\frac{1}{\tau_{nr}}+\frac{1}{\tau_r}\right)^{-1}, \tag{3}$$

where $1/\tau_r$ and $1/\tau_{nr}$ are the total radiative and nonradiative transition rates, respectively. The total nonradiative rate, $1/\tau_{nr}$, is given by

$$\frac{1}{\tau_{nr}}=\frac{1}{\tau_{LO}}+\frac{1}{\tau_{AC}}+\frac{1}{\tau_{ee}}, \tag{4}$$

where $1/\tau_{LO}$, $1/\tau_{AC}$, and $1/\tau_{ee}$ are the longitudinal optical (LO) phonon, acoustic (AC) phonon, and electron–electron scattering rates, respectively. Quantum efficiencies were calculated for each value of electric field at temperatures of 4, 77, and 300 K. A carrier concentration of 1×10^{10} cm^{-2} was assumed for these calculations. Self-consistent Schrödinger–Poisson calculations on similar quantum well systems have demonstrated that the band bending at these low carrier densities is negligible (<1 meV).[15] The radiative and nonradiative transition rates vary with electron density, although the radiative rates do not vary appreciably with temperature. Therefore for a field of 32 kV cm^{-1} and a temperature of 4

TABLE II. Scattering rates at 300 K with an applied field of 40 kV cm^{-1}.

Transition	$1/\tau_{LO}$	$1/\tau_{AC}$	$1/\tau_{ee}$
$5\rightarrow4$	2.457×10^{11}	2.784×10^{9}	8.636×10^{7}
$4\rightarrow3$	2.452×10^{11}	2.763×10^{9}	8.573×10^{7}
$3\rightarrow2$	2.447×10^{11}	2.754×10^{9}	8.534×10^{7}
$2\rightarrow1$	2.372×10^{11}	2.666×10^{9}	8.096×10^{7}

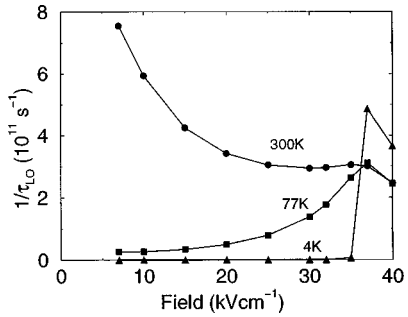

FIG. 3. Interwell LO phonon scattering rates for the Stark ladder as a function of the electric field.

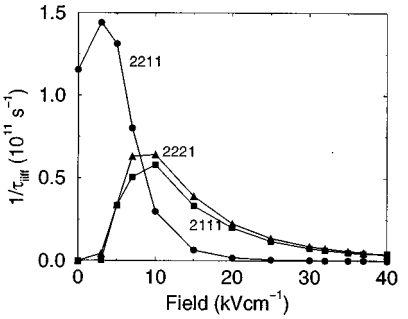

FIG. 5. Individual electron–electron scattering rates at 4 K, showing the three mechanisms by which interwell electron–electron transitions can take place.

K, the radiative and nonradiative transition rates were calculated for different carrier concentrations (from 5×10^{9} to 1×10^{11} cm^{-2}) and the quantum efficiency was calculated for each case.

III. RESULTS AND DISCUSSION

Figures 3–6 show graphs of LO phonon, acoustic phonon, and electron–electron scattering rates as a function of increasing electric field. Scattering rates are shown at different temperatures to determine the conditions under which losses are minimized and at which nonradiative processes are dominant. Data are shown only for fields greater than 7 kV cm^{-1}. This represents the point of Stark ladder formation. Below this field the system is in the ''mini-band breakup'' region which is not appropriate for emitter applications.

It can be seen that at a temperature of 4 K no LO phonon transitions take place for electric fields below 36 kV cm^{-1} because the intersubband separation for these fields is less than the LO phonon energy. At a field of 36 kV cm^{-1}, the intersubband separation is equal to the LO phonon energy and LO phonon scattering becomes effective. At 77 K the LO phonon scattering rate peaks at a field of 36 kV cm^{-1}, corresponding to a resonance at the LO phonon energy. However, the peak is not as large as that at 4 K because there is a slight thermal broadening, causing some of the electrons to have energies greater than the LO phonon energy. At 300 K, the thermal energy of the system is $kT\approx26$ meV and this causes substantial thermal broadening of the electron distribution function. Consequently, there are many electrons having sufficient energy to emit a LO phonon, so the LO scattering rate is high at low fields, even though the intersubband separation is much lower than 36 meV. As the field is increased, the states become more localized, hence the wave function overlap decreases. The probability of an electron scattering into a lower state is therefore reduced, resulting in a lower LO phonon scattering rate at higher fields.

The AC phonon scattering rate decreases as the electric field is increased and is not very significant at 4 and 77 K, except at low fields. The AC phonon interaction strength is proportional to the energy of the emitted phonon, so at low fields, where the intersubband separation is small, the AC phonon transition rate is higher. At its peak rate at a temperature of 300 K and a field of 5 kV cm^{-1}, the AC scattering rate is about 5% of the LO rate.

The graph of individual electron–electron scattering rates from level 2 to level 1 at 4 K (Fig. 5) shows that the Auger-type processes are not as significant as the transitions where both electrons are scattered from level 2 to level 1 (2211) until a field of 10 kV cm^{-1} is applied. The rates for Auger processes 2111 and 2221 are about 60% and 75%, respectively, of the rate of the non-Auger process 2211 at 7 kV cm^{-1}. Indeed, the selection rule forbidding Auger-type processes at zero field arises naturally from the results of the calculations, as can be seen from Fig. 5. There needs to be a large enough field to antisymmetrize the electron wave functions and, when this field is attained, the Auger scattering processes can become dominant. All the electron–electron scattering rates decrease with increasing field, as illustrated in Fig. 6, because, as the electrons gain more energy, a larger momentum change is needed for an intersubband scattering

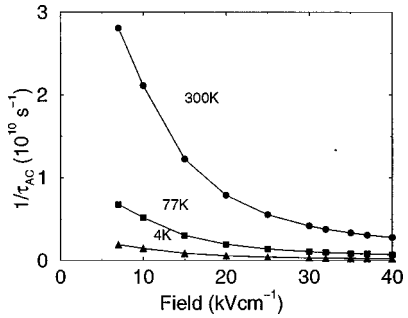

FIG. 4. Interwell AC phonon scattering rates for the Stark ladder as a function of the field.

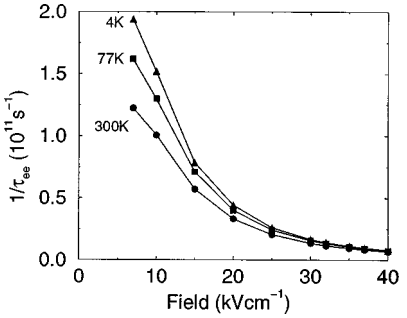

FIG. 6. The total interwell electron–electron scattering rates at 4, 77 and 300 K.

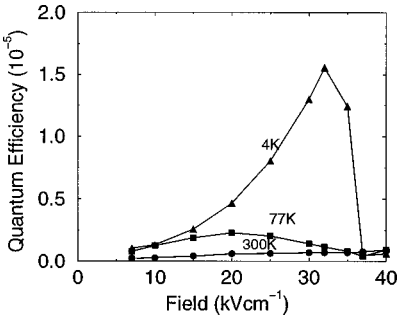

FIG. 7. Quantum efficiency as a function of field at 4, 77, and 300 K.

event to take place. The probability of electron–electron scattering decreases as a larger field is applied and the electrons gain momentum. At low fields the electron–electron scattering rate at 4 K is about 40% greater than that at 300 K and 20% greater than the electron–electron scattering rate at 77 K. This is because the Fermi–Dirac distribution at low temperatures is such that there is a greater probability of an electron occupying a state near the Fermi energy.

The quantum efficiency of the system is shown in Fig. 7. It can be seen that the quantum efficiency is low ($\sim 1 \times 10^{-5}$) at low fields for all values of temperature. However, at 4 K the quantum efficiency peaks at a field of 32 kV cm^{-1} and has a value of 1.555×10^{-5}. This is because the most significant loss mechanism, LO phonon scattering, is suppressed at 4 K below fields of 36 kV cm^{-1}. The AC phonon and electron–electron scattering rates also decrease substantially as the field is increased to this value. Although $\sim 2 \times 10^{-5}$ would appear to be a low quantum efficiency, it should be considered that 2×10^{-5} photons are emitted every time an electron is scattered from well $m+1$ to well m. For a typical superlattice having 100 repeats this would give 2×10^{-3} photons per electron, which approaches an acceptable output. It can be seen that the quantum efficiency decreases at longer wavelengths. The maximum wavelength for $F = 7$ kV cm^{-1} is 177 μm, and the quantum efficiency here has decreased by a factor of 10 from its peak value, which occurs at a field of 32 kV cm^{-1} (corresponding to a wavelength of 38 μm).

At 77 K the peak in quantum efficiency is a factor of 8 less than the peak at 4 K, and the peak at 300 K is a factor of 20 less than that at 4 K. Both these peaks occur at a field of 20 meV, corresponding to a wavelength of 62 μm.

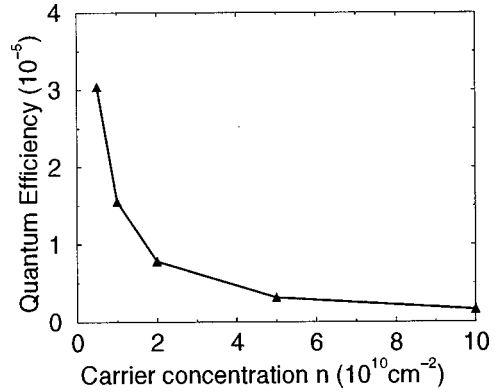

FIG. 8. Quantum efficiency as a function of carrier concentration for an electric field of 32 kV cm^{-1} and a temperature of 4 K.

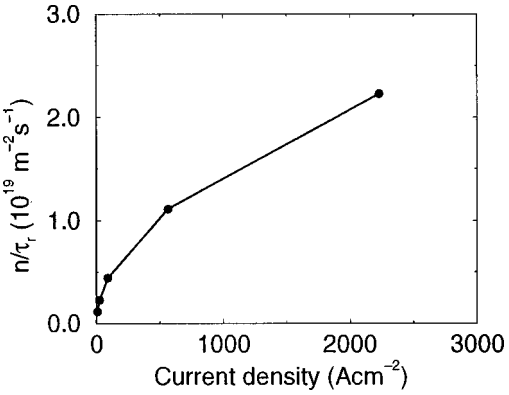

FIG. 9. Emitted photon density per well for an electric field of 32 kV cm^{-1} and a temperature of 4 K.

In Fig. 8 the quantum efficiency is shown as a function of varying carrier concentration. The quantum efficiency decreases with increasing carrier concentration, as a direct result of increased electron–electron scattering.

Figure 9 shows the number of photons per well per unit area per unit time (given by n/τ_r) as a function of current density, J, which is given by

$$J = \frac{ne}{\tau_{nr}}. \tag{5}$$

At a field of 32 kV cm^{-1}, with a carrier concentration of $n = 10^{10}$ cm^{-2}, the current density is 2.2×10^3 A cm^{-2} and there are 2.2×10^{19} photons emitted per well per unit area per second. For a typical device having 100 wells of area 1 cm^2, the power output would be approximately 1.1 mW, which approaches useful levels.

IV. CONCLUSIONS

Calculations of intersubband transition rates by both radiative and nonradiative processes indicate the potential of a Stark ladder based on GaAs technology for tunable far-infrared emission. The range of output wavelengths for the design advanced here would be tunable from 38 to 177 μm, with a maximum efficiency at a temperature of 4 K in the shorter wavelength region.

ACKNOWLEDGMENTS

The authors would like to thank the School of Electronic and Electrical Engineering and the University of Leeds for financial support.

[1] J. Faist, F. Capasso, C. Sitori, D. I. Sivco, A. L. Hutchinson, and A. Cho, Appl. Phys. Lett. **67**, 3057 (1995).
[2] G. Scarmarcio, F. Capasso, J. Faist, C. Sirtori, D. L. Sivco, and A. L. Hutchinson, Appl. Phys. Lett. **70**, 1796 (1997).
[3] B. Xu, Q. Hu, and M. R. Melloch, Appl. Phys. Lett. **71**, 440 (1997).
[4] P. Harrison, in *New Directions in Terahertz Technology*, edited by J. M. Chamberlain and R. E. Miles (Kluwer, Amsterdam, 1997), p. 130.
[5] *Carrier Scattering in Metals and Semiconductors*, edited by V. F. Gantmakher and Y. B. Levinson (Elsevier, Amsterdam, 1987).
[6] P. Harrison and R. W. Kelsall, J. Appl. Phys. **81**, 7135 (1997).
[7] P. Harrison, Semicond. Sci. Technol. **12**, 1487 (1997).

[8] R. G. Roberts, P. Harrison, T. Stirner, and W. E. Hagston, J. Phys. II **3**, 203 (1993).
[9] A. Goswami, *Quantum Mechanics* (Brown, Dubuque, 1992)
[10] P. Harrison, W. E. Hagston, and T. Stirner, Phys. Rev. B **47**, 16404 (1993).
[11] S. Adachi, *GaAs and Related Materials* (World Scientific, Singapore, 1994).
[12] J. H. Smet, C. G. Fonstad, and Q. Hu, J. Appl. Phys. **79**, 9305 (1996).
[13] E. L. Ivchenko and G. E. Pikus, *Superlattices and Other Heterostructures* (Springer, Berlin, 1997).
[14] P. Kinsler, P. Harrison, and R. W. Kelsall, Phys. Rev. B **58**, 4771 (1998).
[15] P. Harrison (unpublished).